Received: 10 October 2023 | Revised: 17 November 2023 | Accepted: 2 December 2023

IET Radar, Sonar & Navigation

DOI: 10.1049/rsn2.12526

The Institution of Engineering and Technology WILEY

ORIGINAL RESEARCH

Robust localisation methods based on modified skipped filter weighted least squares algorithm

Chee-Hyun Park | **Joon-Hyuk Chang**

Electronic Engineering, Hanyang University, Seoul, Korea

Correspondence
Joon-Hyuk Chang.
Email: jchang@hanyang.ac.kr

Funding information
Korea Government, Grant/Award Number: No.2021-0-00456

Abstract

Robust localisation techniques that utilise distance observations to determine the location are focused upon. In urban environments with limited visibility and high population density, the presence of non-line-of-sight signals can introduce a positive measurement bias, negatively affecting the accuracy of estimation. To resolve this problem caused by multipath effects, robust localisation techniques have been explored, specifically the skipped filter weighted least squares (WLS) method for localisation. However, the squared estimation bias of the transformed distance estimate of the existing skipped filter WLS method is high in the low signal-to-noise ratio condition owing to the second-order noise terms. Therefore, the modified skipped filter WLS methods are proposed to reduce the squared estimation bias of transformed distance estimate. First, the closed-form modified skipped filter WLS method uses the maximum likelihood estimate (MLE) to reduce the squared estimation bias of the transformed distance estimate. In addition, the modified skipped filter WLS method using the online ML and online expectation maximisation (EM) algorithms are introduced whose advantage is that they do not require the number of Gaussian components unlike the existing Gaussian mixture model EM algorithm. The mean square error analysis of proposed closed-form skipped filter WLS and existing skipped filter WLS methods is performed. Furthermore, the localisation accuracy of the proposed techniques is found to outperform that of competing algorithms via simulation results.

KEYWORDS
parameter estimation, signal processing

1 | INTRODUCTION

Accurate and reliable localisation of objects and devices has become increasingly important across various fields, including wireless communication, robotics, and navigation systems. Time-of-arrival (TOA) localisation is a popular technique that estimates the position of a target by measuring the time it takes for a signal to travel from a transmitter to the receiver. However, TOA localisation is prone to various challenges, such as multipath propagation, interference, and non-line-of-sight (NLOS) conditions, which can significantly degrade its accuracy and reliability. Therefore, it is essential to create an algorithm that solves the aforementioned issues for localisation using TOA measurements. Specifically, the focus of this study is to devise an accurate method dealing with NLOS noise for determining the position of the target node.

In the context of localisation, extensive studies have been conducted on LOS scenarios [1–6]; however, research on NLOS situations is relatively limited. Previous studies have explored various approaches, including convex optimisation [7–11], robust statistics [12–19], LOS and NLOS sensor identification [20–22], and robust filtering [23–33], to estimate location under NLOS conditions. Although the maximum likelihood estimator (MLE) is well known for its efficiency, it may not be practical when attempting to estimate the parameters of the LOS/NLOS mixed model using MLE due to the time-variant characteristics of NLOS noise statistics. Recently, the maximal correntropy criterion (MCC) has gained attention as an outlier-resistant method [27–29]. Robust Kalman filters have shown superior performance over traditional Kalman filters and unscented Kalman filters in mixed LOS/NLOS scenarios [27–29]. Additionally, a novel algorithm known as the generalised maximum correntropy (GMCC) Kalman filter is introduced [33], offering effective mitigation of NLOS errors. However, the usage of a small kernel bandwidth can render the MCC-based technique unstable and prone to divergence. Furthermore, the determination of the tuning parameters and covariance matrix is not an easy task because they are generally found by trial and error. Another method is a robust localization approach that utilises probability density function (PDF) estimation. It estimates the LOS distance by identifying the support for the first peak [34]. The underlying principle of this method is that the direct LOS path always results in a shorter distance measurement compared to the indirect NLOS path. Despite the high accuracy of the robust localisation based on the PDF estimation method, this method is proper for the localisation of the static or slowly moving object because the computational complexity is high. To enable vehicle positioning in challenging environments such as the fast moving object scenarios, a localisation algorithm is designed based on multi-epoch and multi-antenna TOA observations. This algorithm incorporates TOAs from recent multiple epochs and introduces inter-epoch constraints on position and attitude changes [35]. To resolve the ranging problem, a Bayesian approach is proposed [36]. Furthermore, the Euclidean distance matrix is employed to locate multiple sources [37]. In addition, a number of studies have been proposed to reduce the bias in localization when the measurement noise is large [38–41].

A closed-form skipped filter weighted least squares (WLS) method (CS-WLS) has been developed to attenuate the adverse effects of NLOS noise [15, 16]. However, the squared estimation bias of this method is large. Accordingly, the MLE is used to estimate the transformed distance. Consequently, the squared estimation bias of the MLE for the transformed distance becomes smaller than that of the existing skipped filter WLS method. This reduced squared estimation bias of the proposed closed-form modified skipped filter WLS (CMS-WLS) method renders the mean square error (MSE) smaller than that of the existing CS-WLS method. In addition, the Gaussian mixture model (GMM)-based expectation maximisation (EM) algorithm has been used for emitter localization. However, the disadvantage of this algorithm is that it requires the number of Gaussian components. This information cannot be obtained easily a priori in most practical situations. To resolve this problem, the Gaussian mixture distribution is approximated as a single component Gaussian distribution. Then, online methods are utilised because the PDF changes at each time instant. Additionally, the MLE is used to maintain the optimal estimation performance; that is, online maximum likelihood (ML) and EM algorithms are employed to attain the optimal performance without knowing the number of Gaussian components.

The key contributions of this study are summarised as follows:

- The CMS-WLS method is developed to lower the squared estimation bias of the existing CS-WLS method. The transformed distance is estimated using the MLE instead of the sample mean because the squared estimation bias of the transformed distance estimate based on the MLE is smaller than that of the transformed distance estimate using the sample mean (note that the MSE is the sum of the squared estimation bias and error variance).
- The MSE analysis of the CMS-WLS method is performed. The MSE of the proposed CMS-WLS method is shown to be smaller than that of the existing CS-WLS method because the squared estimation bias of the former is smaller than that of the latter.
- A modified skipped filter WLS method based on the online ML algorithm (OMMS-WLS) and a modified skipped filter WLS method based on the online EM algorithm (OEMS-WLS) are devised. The misidentification of the number of Gaussian components renders the estimation error large. Therefore, the knowledge of Gaussian components is important. However, this information cannot be obtained easily in most practical situations. These methods are formulated to develop an algorithm that does not require prior knowledge of the number of Gaussian components. Namely, the single Gaussian component is postulated in the OMMS-WLS and OEMS-WLS methods to overcome the weakness of the existing GMM-EM method. Hence, these proposed algorithms differ from the existing GMM-EM algorithm which needs the accurate number of Gaussian components in this regard.
- The MSEs of the distance estimate of the proposed online algorithms are shown to be smaller than that of the skipped filter WLS method using the existing GMM EM (GMMS-WLS) algorithm. Subsequently, overall positioning MSEs of the proposed online algorithms are smaller than that of the existing GMMS-WLS algorithm.

The subsequent sections of this study are organised as follows. Section II outlines the problem of location estimation in mixed LOS/NLOS scenarios. In Section III, the modified skipped filter WLS localisation approaches proposed in this study are introduced. The theoretical analysis of the MSE of the CMS-WLS and CS-WLS methods is provided in Section IV. The performance evaluation is presented in Section V, where the root mean square error (RMSE) performance is assessed based on simulation results. Lastly, Section VI concludes the paper and discusses potential future directions.

2 | PROBLEM FORMULATION

The goal of the emitter localisation method is to find the solution that achieves the lowest value of the risk function. More specifically, robust techniques aim to identify and mitigate the effects of outliers. These robust methods can suppress or eliminate unwanted signal components and improve the accuracy of TOA measurements. In scenarios dealing with the localisation of a source under mixed LOS and NLOS conditions, the measurement equation is shown as

$$\begin{aligned} r_{i,j} &= d_i + n_{i,j} \\ &= \sqrt{(x - x_i)^2 + (y - y_i)^2} + n_{i,j}, \end{aligned} \tag{1}$$

where $[x_i \; y_i]^T$ represents the known Cartesian coordinates of the ith sensor, whereas $[x \; y]^T$ denotes the unknown position of the target node. Moreover, $r_{i,j}$ represents the range observation from the target node to the ith sensor at the jth time instance, and d_i represents the actual distance. Additionally, the variable $n_{i,j}$ represents a two-mode Gaussian mixture random variable defined as a combination of two Gaussian distributions: $(1-\nu_i)\mathcal{N}(0, \sigma_1^2) + \nu_i \mathcal{N}(\mu_{i,2}, \sigma_2^2)$. Here, $i = 1, 2, \ldots, M$ refers to the number of sensors, and $j = 1, 2, \ldots, P$ refers to the number of observations in each sensor. In this mixture model, the inliers follow a Gaussian distribution with a mean and variance of 0 and σ_1^2, respectively. The outliers follow a Gaussian distribution with a mean and variance of $\mu_{i,2}$ and σ_2^2, respectively. Parameter ν_i represents the contamination ratio, which typically takes values between 0 and 1. Notably, ν_i is typically lower than 0.5, except for heavily NLOS contaminated scenarios. The two-mode GMM has been widely used to model scenarios involving mixed LOS and NLOS conditions [23–26]. However, in practical scenarios, obtaining precise information regarding the statistical moments of the NLOS noise distribution may be infeasible. To assess the robustness of the proposed localisation algorithms against modelling errors, computer simulations are conducted. These algorithms are compared with state-of-the-art techniques under various NLOS error models. By squaring both sides of Equation (1) and rearranging the terms, the following expression is derived:

$$\begin{aligned} x_i x + y_i y - 0.5R + m_{i,j} = 0.5\left(x_i{}^2 + y_i{}^2 - r_{i,j}^2\right), \\ i = 1, 2, \ldots, M, \quad j = 1, 2, \ldots, P \end{aligned} \tag{2}$$

where $R = x^2 + y^2, m_{i,j} = -d_i n_{i,j} - \frac{1}{2} n_{i,j}^2$. Furthermore, the following expression is obtained by representing Equation (2) in a matrix form

$$\mathbf{A}\mathbf{x} + \mathbf{m}_j = \mathbf{b}_j, \qquad j = 1, \ldots, P \tag{3}$$

where $\mathbf{m}_j = [m_{1,j}, \ldots, m_{M,j}]^T$, $\mathbf{x} = [x \; y \; R\,]^T$,

$$\mathbf{A} = \begin{pmatrix} x_1 & y_1 & -0.5 \\ \vdots & \vdots & \vdots \\ x_M & y_M & -0.5 \end{pmatrix} \tag{4}$$

$$\text{and } \mathbf{b}_j = [b_{1,j} \cdots b_{M,j}]^T = \frac{1}{2} \begin{pmatrix} x_1^2 + y_1^2 - r_{1,j}^2 \\ \vdots \\ x_M^2 + y_M^2 - r_{M,j}^2 \end{pmatrix}. \tag{5}$$

The objective is to determine the unknown location parameter x by effectively combining the transformed distance observations, $[\mathbf{b}_1, \ldots, \mathbf{b}_P]$. The commonly used approach for this purpose is the two-step WLS method, which is preferred due to its simplicity. This study utilises uppercase bold letters to denote matrices and lowercase bold letters to represent vectors. The transpose operation is indicated by the operator $[\cdot]^T$.

3 | PROPOSED METHODS

This section presents the proposed CMS-WLS method. Furthermore, the OMMS-WLS and OEMS-WLS algorithms are introduced.

3.1 | CMS-WLS method

The CMS-WLS algorithm based on the invariance property of the MLE is presented. The invariance property of MLE refers to a property of MLE that if $\hat{\theta}$ is the MLE of θ, then $g\hat{\theta}$ is the MLE of $\eta = g(\theta)$ [42]. In addition, $g(\theta)$ must be a one-to-one function. The transformed distance estimate of the existing skipped filter WLS method, defined as $\mu_{b_i,1}^{\text{CS}}$ (the superscript CS is the abbreviation of the closed-form skipped filter), was obtained as follows [15, 16]:

$$\mu_{b_i,1}^{\text{CS}} = \frac{1}{P_{\text{LOS}}} \sum_{j \in \text{LOS}} b_{i,j} \tag{6}$$

$$\begin{aligned} b_{i,j} &= \frac{x_i^2 + y_i^2 - r_{i,j}^2}{2} \\ i &= 1, 2, \ldots, M \end{aligned} \tag{7}$$

where P_{LOS} denotes the number of observations that are predicted as LOS samples via Rao-testing [43], which indicates that the corresponding sample is an outlier when the following condition is satisfied:

$$\begin{aligned} T_R(r_{i,j}) = \frac{(r_{i,j} - d_i)^2}{\sigma_1^2} > \gamma \\ i = 1, 2, \ldots, M, \quad j = 1, 2, \ldots, P \end{aligned} \tag{8}$$

where the threshold (γ) is determined by the α-level rule. In addition, d_i is estimated in Equation (8) as follows. First, the position estimate is obtained based on the least squares method using the median of transformed distances. Then, d_i is calculated using this position estimate. However, $\mu^{CS}_{b_i,1}$ is not optimal in terms of any error measure, such as the sum of squares or likelihood function. This estimate approximates the optimal estimate in the sufficiently small noise conditions, but is not optimal in the large noise conditions owing to the second-order noise term. Accordingly, $\mu^{CS}_{b_i,1}$ is modified such that it is equal to the MLE because the MLE is an asymptotically optimal estimator. The transformed distance estimate in the CMS-WLS method, defined as $\mu^{CMS}_{b_i,1}$ (the superscript CMS denotes the abbreviation of the closed-form modified skipped filter), is obtained by the invariance property of the MLE as follows:

$$\mu^{CMS}_{b_i,1} = \frac{x_i^2 + y_i^2 - (\hat{r}_i\text{MLE})^2}{2} \tag{9}$$

$$\hat{r}_i\text{MLE} = \frac{1}{P_{LOS}} \sum_{j\in LOS} r_{i,j} \tag{10}$$

$$i = 1, 2, \ldots, M.$$

Then, the first-step WLS solution is obtained as follows [2, 3]:

$$\hat{\mathbf{x}} = \left(\mathbf{A}^T \left(\mathbf{C}^{CMS}_{\boldsymbol{\mu}_{b,1}}\right)^{-1} \mathbf{A}\right)^{-1} \mathbf{A}^T \left(\mathbf{C}^{CMS}_{\boldsymbol{\mu}_{b,1}}\right)^{-1} \boldsymbol{\mu}^{CMS}_{b,1} \tag{11}$$

where $\boldsymbol{\mu}^{CMS}_{b,1} = \left[\mu^{CMS}_{b_1,1}, \ldots, \mu^{CMS}_{b_M,1}\right]^T$, $\mu^{CMS}_{b_i,1} = \frac{x_i^2+y_i^2-(\hat{r}_i\text{MLE})^2}{2}$, $\mathbf{C}^{CMS}_{\boldsymbol{\mu}_{b,1}} = \text{diag}\left[\left(\sigma_{\mu_{b_1,1}}{}^2\right)^{CMS}, \ldots, \left(\sigma_{\mu_{b_M,1}}{}^2\right)^{CMS}\right]$, $\left(\sigma_{\mu_{b_i,1}}{}^2\right)^{CMS} \simeq \frac{d_i^2\sigma_1^2}{P_{LOS}} \simeq \frac{(\hat{r}_i\text{MLE})^2 \hat{\sigma}_{i,1}2}{P_{LOS}}$, where $\hat{\sigma}_{i,1}2 = \frac{\sum_{j\in LOS}(r_{i,j} - \hat{r}_i\text{MLE})^2}{P_{LOS}}$ and the second-order noise terms are neglected in the calculation of error variances. Also, the second-step estimate is expressed as follows [2, 3]:

$$\hat{\mathbf{x}}_s = \left(\mathbf{H}^T \mathbf{C}_{\hat{\mathbf{h}}}^{-1} \mathbf{H}\right)^{-1} \mathbf{H}^T \mathbf{C}_{\hat{\mathbf{h}}}^{-1} \hat{\mathbf{h}} \tag{12}$$

where the subscript s denotes the second-step estimate,

$$\hat{\mathbf{h}} = \left[[\hat{\mathbf{x}}]_1^2 \; [\hat{\mathbf{x}}]_2^2 \; [\hat{\mathbf{x}}]_3\right]^T, \tag{13}$$

$$\mathbf{H} = \begin{pmatrix} 1 & 0 \\ 0 & 1 \\ 1 & 1 \end{pmatrix}, \tag{14}$$

$$\mathbf{C}\hat{\mathbf{h}} = \text{diag}[2x \; 2y \; 1]\left(\mathbf{A}^T \left(\mathbf{C}^{CMS}_{\boldsymbol{\mu}_{b,1}}\right)^{-1} \mathbf{A}\right)^{-1} \text{diag}[2x \; 2y \; 1] \simeq \text{diag}\left[2[\hat{\mathbf{x}}]_1 \; 2\hat{\mathbf{x}}_2 \; 1\right]\left(\mathbf{A}^T \left(\mathbf{C}^{CMS}_{\boldsymbol{\mu}_{b,1}}\right)^{-1} \mathbf{A}\right)^{-1} \text{diag}\left[2[\hat{\mathbf{x}}]_1 \; 2[\hat{\mathbf{x}}]_2 \; 1\right], \tag{15}$$

and $[\hat{\mathbf{x}}]_i$ ($i = 1,2,3$) is the ith component of $\hat{\mathbf{x}}$. The final emitter position estimate can be expressed as follows [2, 3]:

$$\hat{\mathbf{x}}_f = \left[\text{sgn}\left([\hat{\mathbf{x}}]_1\right)\sqrt{[\hat{\mathbf{x}}_s]_1} \quad \text{sgn}(\hat{\mathbf{x}}_2)\sqrt{[\hat{\mathbf{x}}_s]_2}\right]^T \tag{16}$$

where sgn $(\cdot)$ indicates the sign function and $[\hat{\mathbf{x}}_s]_i$ ($i = 1,2$) is the ith component of the second-step position estimate. The superiority of the MSE performance of the CMS-WLS method compared with that of the existing CS-WLS method is shown in Section IV. A. Note that the CMS-WLS method is the closed-form method. Therefore, the divergence and initialisation problems do not exist. In addition, the computational complexity is lower compared with the iterative methods.

Remark 1. Note that $\mu^{CMS}_{b_i,1}$ is an exactly sufficient statistic because $\hat{r}_i$MLE is a sufficient statistic of d_i and $\mu^{CMS}_{b_i,1}$ is a function of $\hat{r}_i$MLE (any one-to-one function of the sufficient statistic is also the sufficient statistic). In contrast, $\mu^{CS}_{b_i,1}$ is an approximately sufficient statistic [16]. Further, the biases of both statistics are non-zero and this non-zero bias renders the positioning MSE greater than that obtained using the unbiased statistic. Indeed, MSEs of both algorithms would be more degraded than the Cramér-Rao lower bound (CRLB) as the standard deviation of measurement noise (σ_1) increases. However, the positioning MSE obtained using $\mu^{CMS}_{b_i,1}$ is smaller than that obtained employing $\mu^{CS}_{b_i,1}$ because the squared estimation bias of $\mu^{CMS}_{b_i,1}$ is lower than that obtained using $\mu^{CS}_{b_i,1}$ as seen by Equations (30–41).

3.2 | OMMS-WLS method

The main drawback of the standard GMM EM method is that it requires the knowledge of the number of Gaussian components. For example, assume that the user misidentifies the number of Gaussian components are three although the true number is two. Then, the estimation error becomes large due to the misidentification. Therefore, the accurate prediction of the Gaussian components is very important. However, the number of Gaussian components cannot be known easily a priori in most practical situations. Therefore, this problem is resolved by assuming that the observation belongs to only one Gaussian component at each time instant. Consequently, knowing the number of components is not necessary. The GMM at each time instant is represented as follows:

$$L_{i,j} = \sum_{k=1}^{K}\left(\frac{\sqrt{\tau_{i,k}}}{\sqrt{2\pi}} \exp\left(-\frac{\tau_{i,k}}{2}\left(r_{i,j} - d_i - b_{i,k}\right)^2\right)\pi_{i,k}\right)$$

$$j = 1, \ldots, P, i = 1, \ldots, M \tag{17}$$

where $\tau_{i,k}$ denotes the precision parameter of the kth component of the GMM in the ith sensor, d_i is the actual distance between the emitter and the ith sensor, $b_{i,k}$ is the measurement bias of the kth component of the GMM in the ith sensor and $\pi_{i,k}$ denotes the weighting coefficient of the kth component of the GMM in the ith sensor. When one component among K components at each time instant is assumed to be valid, (17) can be rewritten as follows:

$$L_{i,j} \simeq \frac{\sqrt{\tau_{i,k'(j)}}}{\sqrt{2\pi}} \exp\left(-\frac{\tau_{i,k'(j)}}{2}\left(r_{i,j} - d_i - b_{i,k'(j)}\right)^2\right) \quad j = 1, \ldots, P, \; i = 1, \ldots, M \tag{18}$$

where $k'(j)$ denotes the mixture component (k) to which $r_{i,j}$ belongs. The weighting coefficient ($\pi_{i,k}$) is equal to 1 because the integral of the PDF must be 1. Consequently, the log-likelihood function is obtained as follows:

$$l_{i,j} = \frac{1}{2}\log\tau_{i,k'(j)} - \frac{1}{2}\log 2\pi - \frac{\tau_{i,k'(j)}}{2}\left(r_{i,j} - d_i - b_{i,k'(j)}\right)^2 \quad j = 1, \ldots, P, \; i = 1, \ldots, M. \tag{19}$$

Because the PDF alternates at each time instant, the online method is used. Instead of processing the entire dataset in each iteration, online method updates the model parameters when new data arrives. This allows the algorithm to adapt to changing data distributions and update the model in real-time. In addition, the MLE is employed because it is an asymptotically optimal estimator (i.e., the online MLE is used). The rationale behind online MLE is to update the model parameters iteratively using the observed data and the current estimates of the parameters. When new data arrive, the likelihood function is updated, and the model parameters are adjusted to maximise the updated likelihood. This iterative process enables the model to adapt and learn from the new information without requiring access to the entire dataset. By iteratively applying this update rule, the estimates converge to the ML solution as more data become available. Parameters d_i and $b_{i,k'(j)}$ are obtained by differentiating $l_{i,j}$ and setting its derivative to zero as follows:

$$b_{i,k'(j)} = \max\left\{r_{i,j} - d_i, 0\right\} \tag{20}$$

$$d_i = r_{i,j} - b_{i,k'(j)} \quad j = 1, \ldots, P, \; i = 1, \ldots, M. \tag{21}$$

where max is the operator which selects the larger value among two numbers. This operator appears because the measurement bias $b_{i,k'(j)}$ must be a non-negative value. Equations (20) and (21) are iteratively updated online using the entire measurement set. After d_i is estimated, it is substituted into Equation (8) to identify inliers and outliers. Subsequently, the sample mean of the samples predicted as inliers is calculated using (10) and then the transformed distance estimate is computed using Equation (9). Finally, the position of the emitter is calculated using Equations (11–16).

3.3 | OEMS-WLS method

The GMM can be expressed in batch form to integrate observations up to time instance P as follows:

$$L_i = \prod_{j=1}^{P}\left\{\sum_{k=1}^{K}\left(\pi_{i,k}\frac{\sqrt{\tau_{i,k}}}{\sqrt{2\pi}} \exp\left(-\frac{\tau_{i,k}}{2}\left(r_{i,j} - d_i - b_{i,k}\right)^2\right)\right)\right\} \tag{22}$$

$$\simeq \prod_{j=1}^{P}\left\{\frac{\sqrt{\tau_{i,k'(j)}}}{\sqrt{2\pi}} \exp\left(-\frac{\tau_{i,k'(j)}}{2}\left(r_{i,j} - d_i - b_{i,k'(j)}\right)^2\right)\right\} \tag{23}$$

$$i = 1, \ldots, M.$$

The logarithm of Equation (23) is as follows:

$$l_i = \sum_{j=1}^{P}\left\{\frac{1}{2}\log\tau_{i,k'(j)} - \frac{1}{2}\log 2\pi - \frac{\tau_{i,k'(j)}}{2} \times \left(-\frac{\tau_{i,k'(j)}}{2}\left(r_{i,j} - d_i - b_{i,k'(j)}\right)^2\right)\right\} \quad i = 1, \ldots, M. \tag{24}$$

Differentiating Equation (24) with respect to d_i and setting the derivative to zero yields the following:

$$d_i = \frac{\sum_{j=1}^{P}\tau_{i,k'(j)}\left(r_{i,j} - b_{i,k'(j)}\right)}{\sum_{j=1}^{P}\tau_{i,k'(j)}} \quad i = 1, \ldots, M. \tag{25}$$

As seen from Equation (25), $b_{i,k'(j)}$ and $\tau_{i,k'(j)}$ must be calculated to estimate d_i. The online method is employed because the PDF changes at each time step. Further, the calculation of d_i is not required because it is given by Equation (25). Therefore, the online EM method is used regarding d_i as the latent variable. Subsequently, the E-step is represented as follows:

$$\sum_{j=1}^{P} E_{d_i|r_{i,j},\Theta^{(q)}}\left[\log p\left(r_{i,j}, d_i|\Theta\right)\right]$$

$$= \sum_{j=1}^{P}\left(\frac{1}{2}\log\tau_{i,k'(j)} - \frac{1}{2}\log 2\pi - \frac{1}{2}\tau_{i,k'(j)}\left(r_{i,j}^2 + E\left[d_i^2|r_{i,j},\Theta^{(q)}\right] + b_{i,k'(j)^2} - 2r_{i,j}E\left[d_i|r_{i,j},\Theta^{(q)}\right] + 2E\left[d_i|r_{i,j},\Theta^{(q)}\right]b_{i,k'(j)} - 2r_{i,j}b_{i,k'(j)}\right)\right) \tag{26}$$

$$i = 1,\ldots,M$$

where $\Theta^{(q)}$ denotes the $\left[b_{i,k'(j)}^{(q)}, \tau_{i,k'(j)}^{(q)}\right]^T$, the superscript (q) denotes the iteration number, $E\left[d_i|r_{i,j},\Theta^{(q)}\right] = r_{i,j} - b_{i,k'(j)}^{(q)}$ and $E\left[d_i^2|r_{i,j},\Theta^{(q)}\right] = \left(r_{i,j} - b_{i,k'(j)}^{(q)}\right)^2 + \frac{1}{\tau_{i,k'(j)}^{(q)}}$. Here, $E\left[d_i|r_{i,j},\Theta^{(q)}\right]$ and $E\left[d_i^2|r_{i,j},\Theta^{(q)}\right]$ are derived assuming the Jeffreys prior for d_i because no information exists regarding d_i. Differentiating (26) with respect to $b_{i,k'(j)}$, $\tau_{i,k'(j)}$ and setting the derivative to zero yield the following solution:

$$b_{i,k'(j)} = \max\left\{r_{i,j} - E\left[d_i|r_{i,j},\Theta^{(q)}\right], 0\right\} \tag{27}$$

$$\tau_{i,k'(j)} = \frac{1}{A} \tag{28}$$

$$A = r_{i,j}^2 + E\left[d_i^2|r_{i,j},\Theta^{(q)}\right] + b_{i,k'(j)}^2 - 2r_{i,j}E\left[d_i|r_{i,j},\Theta^{(q)}\right] + 2E\left[d_i|r_{i,j},\Theta^{(q)}\right]b_{i,k'(j)} - 2r_{i,j}b_{i,k'(j)} \tag{29}$$

$$j = 1,\ldots,P,\ i = 1,\ldots,M.$$

After estimating $\tau_{i,k'(j)}$ and $b_{i,k'(j)}$, they are substituted into (25) to compute d_i. Subsequently, d_i is inserted into (8) to discriminate inliers and outliers. Then, the MLE for the samples predicted as inliers is calculated using Equation (10) and then the transformed distance estimate is computed using Equation (9). Finally, the position of the emitter is calculated using Equations (11)-(16). In Appendix B, the MSEs of the range estimate of the OMMS-WLS and OEMS-WLS algorithms are shown to be smaller than that of the GMMS-WLS method. These lower MSEs of the distance estimates of the online methods render the overall positioning MSEs of the online methods smaller than that of the GMMS-WLS method. This is because d_i is more accurately estimated in the statistical testing step (8) considering that the remaining procedures are the same. As a result, the inliers and outliers are discriminated more accurately.

Remark 2. The convergence property of the online EM method is described in Refs. [44–46]. The online EM method converges to the stationary point when the signal is independent [44]. In Refs. [45, 46], a similar methodology is employed for hidden Markov models (HMM) with discrete hidden data and observations and this approach is extended to incorporate continuous observations in conjunction with discrete HMM. Moreover, Ref. [47] presents an expansion of the methodology to encompass a broader state-space model utilising sequential Monte-Carlo techniques. Further, almost sure convergence of the online MLE to the stationary points of the asymptotic likelihood is proven by assuming regularity results in a Poisson equation and ergodicity of the system [48–50]. A comprehensive theoretical investigation of the online MLE for HMM is presented in Ref. [51]. This analysis covers various aspects, including the rate of convergence of the algorithm.

4 | PERFORMANCE ANALYSIS

4.1 | MSE analysis

This section presents the comparison between the performance of the proposed CMS-WLS and existing CS-WLS algorithms in terms of MSE. First, the general form for the MSE of the localisation algorithm is derived as follows:

$$E\left[\left(\hat{\mathbf{x}}_f - \mathbf{x}\right)^T\left(\hat{\mathbf{x}}_f - \mathbf{x}\right)\right] = E\left[\left(\boldsymbol{\mu}_{b,1} - \mathbf{b}^o\right)^T\mathbf{B}^T\mathbf{B}\left(\boldsymbol{\mu}_{b,1} - \mathbf{b}^o\right)\right] \tag{30}$$

$$= \mathrm{tr}\left(\mathbf{B}E\left[\left(\boldsymbol{\mu}_{b,1} - \mathbf{b}^o\right)\left(\boldsymbol{\mu}_{b,1} - \mathbf{b}^o\right)^T\right]\mathbf{B}^T\right) \tag{31}$$

$$= \mathrm{tr}\left(\mathbf{B}\mathbf{F}\mathbf{B}^T\right) \tag{32}$$

$$= \mathrm{tr}\left(\mathbf{F}\mathbf{B}^T\mathbf{B}\right) \tag{33}$$

$$= \mathrm{tr}(\mathbf{F}\mathbf{B}') \tag{34}$$

$$= \sum_{i=1}^{M}\sum_{l=1}^{M}[\mathbf{F}]_{i,l}[\mathbf{B}']_{l,i} \tag{35}$$

$$= \sum_{i=1}^{M}\left([\mathbf{F}]_{i,i}[\mathbf{B}']_{i,i} + \sum_{l\neq i}[\mathbf{F}]_{i,l}[\mathbf{B}']_{l,i}\right) \tag{36}$$

$$= \sum_{i=1}^{M}[\mathbf{F}]_{i,i}[\mathbf{B}']_{i,i} + \sum_{i=1}^{M}\sum_{l\neq i}[\mathbf{F}]_{i,l}[\mathbf{B}']_{l,i} \tag{37}$$

$$\simeq \sum_{i=1}^{M}[\mathbf{F}]_{i,i}[\mathbf{B}']_{i,i} \tag{38}$$

where $\mathbf{B} = \mathbf{G}\left(\mathbf{A}^T\mathbf{C}_{\boldsymbol{\mu}_{b,1}}^{-1}\mathbf{A}\right)^{-1}\mathbf{A}^T\mathbf{C}_{\boldsymbol{\mu}_{b,1}}^{-1}$, $\mathbf{B}' = \mathbf{B}^T\mathbf{B}$, $\mathbf{G} = \mathbf{D}_2^{-1}\left(\mathbf{H}^T\mathbf{C}_{\widehat{\mathbf{h}}}^{-1}\mathbf{H}\right)^{-1}\mathbf{H}^T\mathbf{C}_{\widehat{\mathbf{h}}}^{-1}\mathbf{D}_1$, $\mathbf{D}_1 = \text{diag}\ [2x\ \ 2y\ \ 1]$, $\mathbf{D}_2 = 2\text{diag}\ [x\ \ y]$, $\mathbf{F} = E\left[\left(\boldsymbol{\mu}_{b,1} - \mathbf{b}^o\right)\left(\boldsymbol{\mu}_{b,1} - \mathbf{b}^o\right)^T\right]$ and $\mathbf{b}^o = \left[b_1^o, \ldots, b_M^o\right]^T$, where b_i^o denotes the true value of b_i ($i = 1, \ldots, M$) $[\mathbf{F}]_{i,l}$ denotes the $(i,l)^{\text{th}}$ component of the square matrix $\mathbf{F}$ and tr $(\cdot)$ denotes the trace of the square matrix. The magnitude of b_i^o is assumed to be sufficiently larger than σ_1^2 in the derivation of Equation (38) (i.e $[\mathbf{F}]_{i,l} \simeq 0$ because $E\left[\mu_{b_i,1}\right] \simeq b_i^o$ in the sufficiently high SNR condition). Furthermore, $[\mathbf{B}'^{\text{CMS}}]_{i,i}$ and $[\mathbf{B}'^{\text{CS}}]_{i,i}$ are identical when $\mathbf{C}_{\boldsymbol{\mu}_{b,1}}^{\text{CMS}}$ and $\mathbf{C}_{\boldsymbol{\mu}_{b,1}}^{\text{CS}}$ are the same, where $[\mathbf{B}'^{\text{CMS}}]_{i,i}$ and $[\mathbf{B}'^{\text{CS}}]_{i,i}$ are $[\mathbf{B}']_{i,i}$ of the CMS-WLS and existing CS-WLS methods, respectively. Unless otherwise stated, the aforementioned notation is used hereafter. As seen from Appendix A, $\mathbf{C}_{\boldsymbol{\mu}_{b,1}}^{\text{CMS}} = \mathbf{C}_{\boldsymbol{\mu}_{b,1}}^{\text{CS}}$ with the following form:

$$\left[\mathbf{C}_{\boldsymbol{\mu}_{b,1}}^{\text{CMS}}\right]_{i,j} = \left[\mathbf{C}_{\boldsymbol{\mu}_{b,1}}^{\text{CS}}\right]_{i,j} = \begin{cases} \dfrac{d_i^2\sigma_1^2}{P_{\text{LOS}}} + \dfrac{\sigma_1^4}{2P_{\text{LOS}}^3}, & \text{if } i = j \\ 0, & \text{if } i \neq j. \end{cases} \tag{39}$$

Then, $[\mathbf{F}]_{i,i}$ is proportional to the MSE of $\hat{\mathbf{x}}_f$. Therefore, $[\mathbf{F}]_{i,i}^{\text{CMS}}$ and $[\mathbf{F}]_{i,i}^{\text{CS}}$ can be used to prove that the MSE of $\hat{\mathbf{x}}_f^{\text{CMS}}$ is smaller than that of $\hat{\mathbf{x}}_f^{\text{CS}}$. $[\mathbf{F}^{\text{CMS}}]_{i,i}$ and $[\mathbf{F}^{\text{CS}}]_{i,i}$ are calculated as follows (details are shown in Appendix A):

$$\left[\mathbf{F}^{\text{CMS}}\right]_{i,i} = \underbrace{\frac{\sigma_1^4}{4P_{\text{LOS}}^2}}_{\text{squared estimation bias}} + \underbrace{\frac{d_i^2\sigma_1^2}{P_{\text{LOS}}} + \frac{\sigma_1^4}{2P_{\text{LOS}}^3}}_{\text{error variance}} \tag{40}$$

$$\left[\mathbf{F}^{\text{CS}}\right]_{i,i} = \underbrace{\frac{\sigma_1^4}{4}}_{\text{squared estimation bias}} + \underbrace{\frac{d_i^2\sigma_1^2}{P_{\text{LOS}}} + \frac{\sigma_1^4}{2P_{\text{LOS}}^3}}_{\text{error variance}}. \tag{41}$$

Clearly, $[\mathbf{F}^{\text{CMS}}]_{i,i}$ is smaller than $[\mathbf{F}^{\text{CS}}]_{i,i}$ because P_{LOS} generally exceeds 1. Therefore, the MSE of the proposed CMS-WLS method is smaller than that of the existing CS-WLS method because the squared estimation bias of $[\mathbf{F}^{\text{CMS}}]_{i,i}$ is smaller than that of $[\mathbf{F}^{\text{CS}}]_{i,i}$.

4.2 | Initialisation strategy

The distance estimate is initialised to the sample mean of $r_{i,j}$ ($i = 1,\cdots,M, j = 1,\cdots,P$) when the OMMS-WLS and OEMS-WLS algorithms are used. Furthermore, the precision estimate is initially set to the inverse of the sample variance of $r_{i,j}$.

5 | SIMULATION RESULTS

This section presents the comparison of the accuracies of the proposed modified skipped filter WLS methods with those of the CS-WLS method [15, 16], adaptive MCC (AMCC) extended Kalman filter (EKF) [28], statistical similarity measure (SSM)-based Kalman filter [32], and GMMS-WLS method [52]. The RMSE for assessing the accuracy of the localization algorithms is defined as follows:

$$\text{RMSE} = \sqrt{\frac{\sum_{i=1}^{10}\sum_{k=1}^{300}\left[\left(\widehat{x}^k(i) - x(i)\right)^2 + \left(\widehat{y}^k(i) - y(i)\right)^2\right]}{10 \times 300}} \tag{42}$$

where $\left[\widehat{x}^k(i), \widehat{y}^k(i)\right]^T$ represents the Cartesian coordinates of the point target node in the ith position set and kth iteration. Additionally, $x(i)$ and $y(i)$ indicate real position coordinates of the emitter at the ith position. Figure 1 illustrates the arrangement of the tested sources and sensors, depicted as asterisks and circles, respectively. As shown in Figure 1 emitters are tested; however, note that this simulation is for a single emitter localisation.

Figure 2 illustrates the RMSEs as a function of the standard deviation of the LOS noise for different number of LOS/NLOS mixture sensors. In Figure 2a, sensors 5, 6, and 7 were considered as LOS/NLOS mixture sensors, while the remaining sensors were LOS sensors. Similarly, in Figure 2b, sensors 4, 5, 6, and 7 were LOS/NLOS mixture sensors, and in Figure 2c, sensors 3, 4, 5, 6, and 7 were LOS/NLOS mixture sensors. As demonstrated in Figure 2a-c, the RMSEs for all localisation techniques increased as the standard deviation of the LOS noise increased. It is worth noting that at low noise levels, the RMSEs of the proposed methods approached the CRLB. Under the mixture density assumption, the integration in the computation of Fisher information is hard to evaluate analytically. Therefore, we used the Monte-Carlo integration to compute the Fisher information matrix [23]. In addition, the proposed CMS-WLS algorithm outperformed the existing CS-

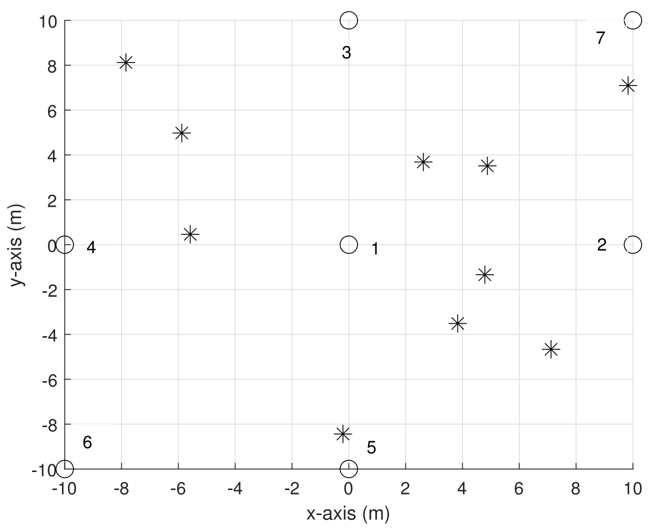

FIGURE 1 The deployment of sensors and sources, where sensors are represented by white circles and sources are denoted by asterisks.

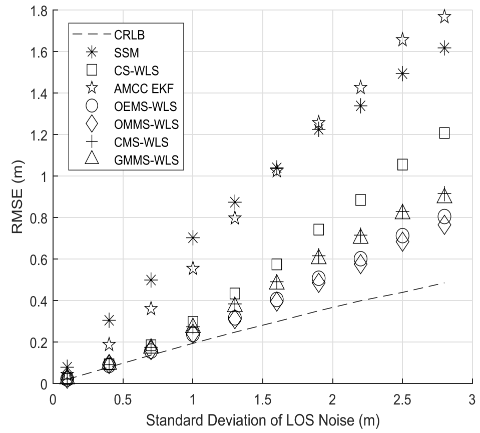

(a)

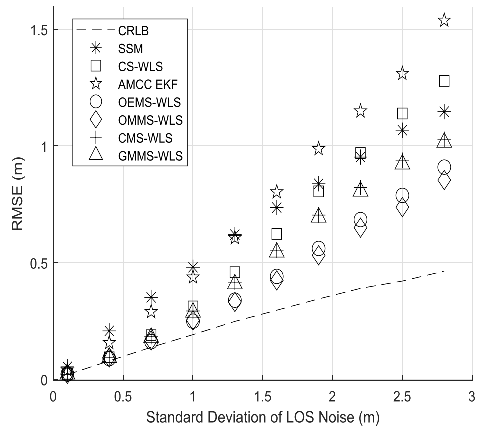

(b)

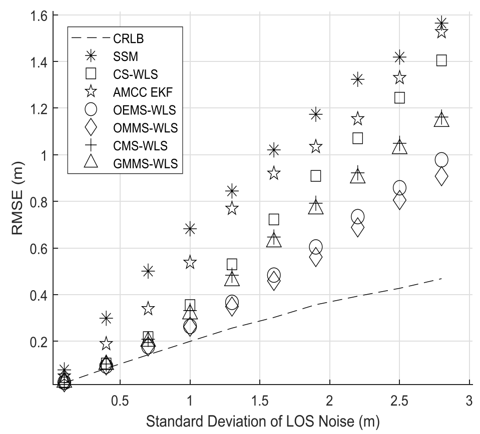

(c)

FIGURE 2 RMSEs of the robust localisation techniques for different levels of LOS noise standard deviation and varying number of the LOS/NLOS mixture sensors. (a) LOS/NLOS mixture sensors: 5, 6 and 7. (b) LOS/NLOS mixture sensors: 4, 5, 6 and 7. (c) LOS/NLOS mixture sensors: 3, 4, 5, 6 and 7.

WLS approach throughout all noise levels. This observation can be explained by Equations (40) and (41); that is, the squared estimation bias of the CMS-WLS method is smaller than that of the existing CS-WLS method. This renders the MSE of the proposed CMS-WLS method smaller than that of the existing CS-WLS method. Moreover, the OEMS-WLS method became more superior to the GMMS-WLS algorithm as the standard deviation of LOS noise increased. Further, the MSE of the OMMS-WLS algorithm was lower than that of OEMS-WLS algorithm and the MSE difference between the two algorithms increased as the standard deviation of measurement noise increased. Although the CMS-WLS method was moderately degraded compared with the OMMS-WLS and OEMS-WLS algorithms, it has no divergence and initialisation problems. Moreover, its computational complexity is lower than that of the counterparts.

Sensors four to seven were considered as LOS/NLOS mixture sensors in Figures 3–5. The RMSEs were shown in Figure 3 as a function of sample size. The accuracy of the proposed methods was higher than that of the other methods, as shown in Figure 3. As the sample size increased, all of the robust approaches improved in performance. The RMSEs of the proposed methods approached the CRLB as the sample size increased. The difference in MSE between the OEMS-WLS and GMMS-WLS algorithms increased with the sample size. The aforementioned observation can be explained in the following manner. When the sample size (P) increases, P_{LOS} would increase with the contamination ratio fixed. Then, $[\mathbf{F}^{\mathrm{OMMS}}]_{i,i}$ and $[\mathbf{F}^{\mathrm{OEMS}}]_{i,i}$ would decrease more rapidly than $[\mathbf{F}^{\mathrm{GMMS}}]_{i,i}$ when the sample size increases, as indicated by Equations (40) and (41)

Figure 4 illustrates the relationship between the contamination ratio and the RMSEs, indicating that the proposed techniques showed relatively consistent RMSEs across different contamination ratios except for a contamination ratio of 1. When the contamination ratio surpassed 0.5, all of the SSM, AMCC EKF, and skipped filter WLS techniques experienced noticeable increments in their RMSEs.

Next, the robustness of the proposed approaches against the NLOS noise modelling mismatch was examined. Despite the formulation of the two-mode GMM in this study, accurately capturing the NLOS error distribution is challenging, leading to potential modelling mismatches. Different noise models, such as the Gaussian-uniform mixture distribution [53, 54], and Gaussian-exponential mixture distribution [55], were considered to evaluate the effectiveness of the proposed algorithms under various NLOS error distributions. Simulation results presented in Figure 5(a),(b) demonstrated that the proposed approaches consistently achieved lower RMSEs compared to conventional methods, even in cases involving the Gaussian-uniform mixture distribution $\mathcal{U}$[0 m, 5 m] and the Gaussian-exponential mixture distribution with a rate parameter of $\frac{1}{4}$.

The RMSEs of d_i in Equation (8) were depicted in Figure 6 as a function of the number of iterations. The RMSEs of the

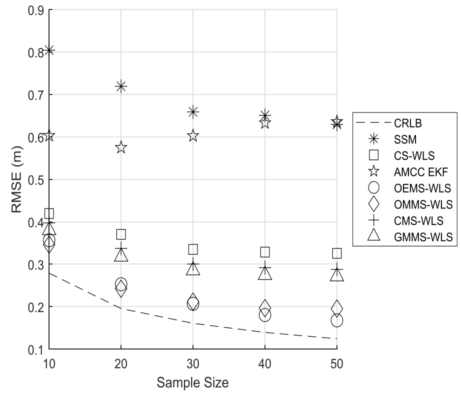

FIGURE 3 RMSEs of various robust localisation methods evaluated across different observation length (σ_2: 3.5 m, σ_1: 1 m, $\nu = 0.4$).

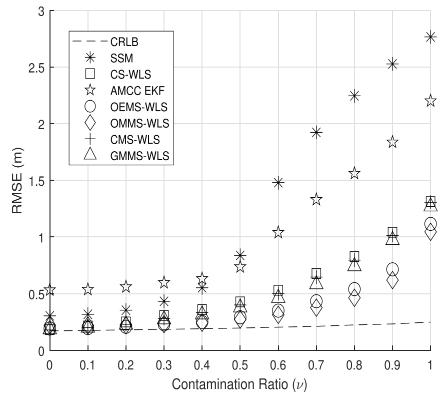

FIGURE 4 RMSEs of various robust localisation methods evaluated across different contamination ratios (ν) (σ_2: 3.5 m, σ_1: 1 m).

proposed online techniques diminished as the number of iterations increased. In addition, the RMSEs of both online methods were lower than that of the existing GMMS-WLS algorithm. Therefore, the overall positioning MSEs of the OMMS-WLS and OEMS-WLS methods were lower than that of other methods because inliers and outliers would be identified more accurately. Furthermore, the RMSE of the OMMS-WLS method converged more rapidly to the stationary state than that of the OEMS-WLS method; however, the RMSEs of both algorithms were similar in the final iteration step. Although the RMSE of the CMS-WLS method was slightly higher than that of the existing GMMS-WLS method, the former has the advantage of being the closed-form algorithm.

The mean square bias (MSB) of the localisation methods was illustrated in Figure 7 as a function of the standard deviation of LOS noise. The MSB is defined as follows:

$$\text{MSB} = \frac{\sum_{i=1}^{10}\left\{\left(\frac{\sum_{k=1}^{300}\hat{x}^{k}(i)}{300} - x(i)\right)^2 + \left(\frac{\sum_{k=1}^{300}\hat{y}^{k}(i)}{300} - y(i)\right)^2\right\}}{10}. \quad (43)$$

As expected, the MSB of the CS-WLS method was higher than that of the CMS-WLS method. In addition, the MSBs of the

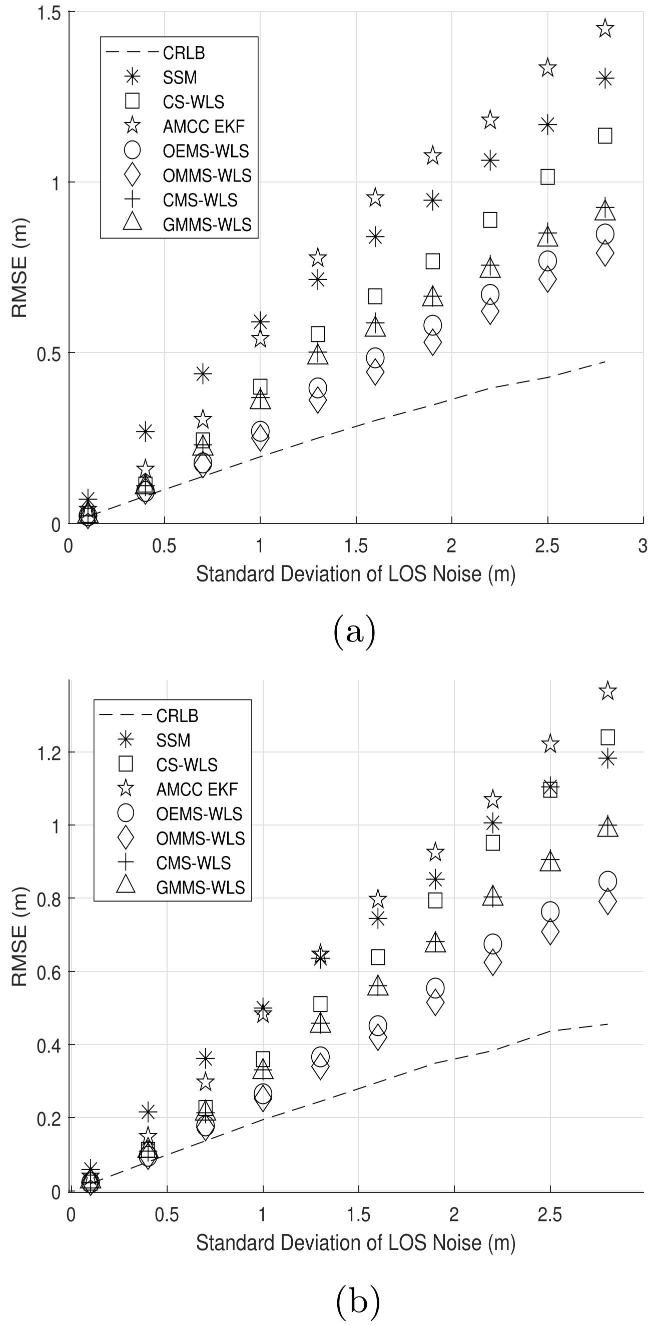

FIGURE 5 RMSEs of various robust localisation techniques as a function of standard deviation of LOS noise assessed for different NLOS error distributions. (a) Gaussian-uniform mixture distribution, NLOS measurement bias: $\mathcal{U}[0\text{ m}, 5\text{ m}]$, $\nu = 0.4$. (b) Gaussian-exponential mixture distribution, NLOS measurement bias: $\text{Exp}\left(\frac{1}{4}\right)$, $\nu = 0.4$.

OMMS-WLS and OEMS-WLS algorithms were the lowest among the localization algorithms and this low MSB renders the overall positioning RMSEs of the online methods lower than those of the other algorithms. However, the MSB of the CMS-WLS method exceeded those of the online methods. The extra bias-reduction method may be used by subtracting the mean of squared error terms from $\mu_{b_i,1}^{\text{CMS}}$ to lower the MSB. Furthermore, the RMSE of the OMMS-WLS method was slightly lower than that of the OEMS-WLS algorithm when the

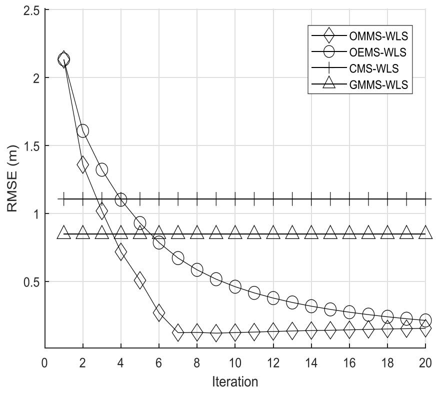

FIGURE 6 RMSEs of d_i in Equation (8) for the robust localisation approaches (σ_2: 3.5 m, σ_1: 0.1 m, $\nu = 0.6$).

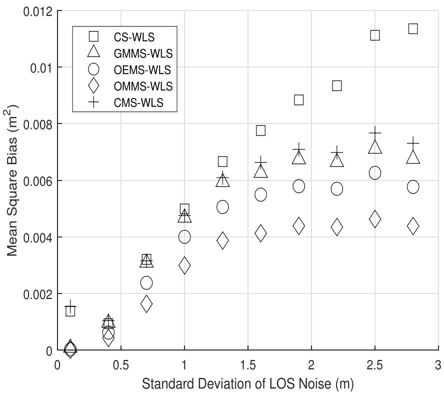

FIGURE 7 Mean square bias of the robust localisation approaches (σ_2: 3.5 m, σ_1: 0.6 m, $\nu = 0.4$).

prior for the range is not known. The OEMS-WLS method may be superior to the OMMS-WLS method when the distribution of the prior for the range is known. However, the range prior cannot be obtained easily and the convergence speed of the EM algorithm is known to be slow. Therefore, it is generally desirable to use the OMMS-WLS method instead of the OEMS-WLS method.

6 | CONCLUSIONS

Modified skipped filter WLS methods were developed in this study. The one is the CMS-WLS method and others are the OMMS-WLS and OEMS-WLS methods. The transformed distance estimate was calculated using the invariance property of the MLE. This technique renders the squared estimation bias of the CMS-WLS method smaller than that of the CS-WLS method in which the transformed distance estimate was calculated using the sample mean. Furthermore, the OMMS-WLS and OEMS-WLS algorithms did not require the number of Gaussian components unlike the existing GMM EM algorithm by assuming that one Gaussian component is valid at each time instant. The MSE analysis for the CMS-WLS and existing CS-WLS methods was performed and the MSE of the CMS-WLS method was proven to be lower than that of the existing CS-WLS algorithm. The simulation results showed the superiority of the proposed methods over existing robust localisation techniques in terms of RMSEs, across different conditions. Subsequent studies will focus on the development of robust localisation algorithm that utilises a single observation.

AUTHOR CONTRIBUTION

Chee-Hyun Park: Conceptualisation; Data curation; Formal analysis; Methodology; Software; Writing – original draft. **Joon-Hyuk Chang**: Funding acquisition; Project administration; Supervision; Writing – review & editing.

ACKNOWLEDGEMENTS

This work was supported by Institute of Information & communications Technology Planning & Evaluation (IITP) grant funded by the Korea government (MSIT) (No.2021-0-00456, Development of Ultra-high Speech Quality Technology for Remote Multi-speaker Conference System).

CONFLICT OF INTEREST STATEMENT

None.

DATA AVAILABILITY STATEMENT

Data available on request from the authors.

ORCID

Chee-Hyun Park https://orcid.org/0000-0002-9739-5277
Joon-Hyuk Chang https://orcid.org/0000-0003-2610-2323

REFERENCES

1. Torrieri, D.J.: Statistical theory of passive location systems. IEEE Trans. Aero. Electron. Syst. 20(2), 183–198 (1983). https://doi.org/10.1109/taes.1984.310439
2. Chan, Y.T., Ho, K.C.: A simple and efficient estimator for hyperbolic location. IEEE Trans. Signal Process. 42(8), 1905–1915 (1994). https://doi.org/10.1109/78.301830
3. So, H.C., Lin, L.: Linear least squares approach for accurate received signal strength based source localization. IEEE Trans. Signal Process. 59(8), 4035–4040 (2011). https://doi.org/10.1109/tsp.2011.2152400
4. Park, C.H., Chang, J.-H.: Closed-form localization for distributed MIMO radar systems using time delay measurements. IEEE Trans. Wireless Commun. 15(2), 1480–1490 (2016). https://doi.org/10.1109/twc.2015.2490677
5. Park, C.H., Chang, J.-H.: Shrinkage estimation-based source localization with minimum mean squared error criterion and minimum bias criterion. Digit. Signal Process. 29, 100–106 (2014). https://doi.org/10.1016/j.dsp.2014.02.009
6. Belloch, J.A., et al.: On the performance of multi-GPU-based expert systems for acoustic localization involving massive microphone arrays. Expert Syst. Appl. 37(8), 5542–5548 (2010). https://doi.org/10.1016/j.eswa.2010.02.059
7. Zhang, S., et al.: Robust NLOS error mitigation method for TOA-based localization via second-order cone relaxation. IEEE Commun. Lett. 19(12), 2210–2213 (2015). https://doi.org/10.1109/lcomm.2015.2482979
8. Wang, G., et al.: NLOS error mitigation for TOA-based localization via convex relaxation. IEEE Trans. Wireless Commun. 13(8), 4119–4131 (2014). https://doi.org/10.1109/twc.2014.2314640

9. Vaghefi, R.M., Schloemann, J., Buehrer, R.M.: NLOS mitigation in TOA-based localization using semidefinite programming. In: Proc. Positioning Navigation and Communication (WPNC), pp. 1–6. Dresden (2013)
10. Vaghefi, R.M., Buehrer, R.M.: Cooperative localization in NLOS environments using semidefinite programming. IEEE Commun. Lett. 19(8), 1382–1385 (2015). https://doi.org/10.1109/lcomm.2015.2442580
11. Tomic, S., Beko, M.: A bisection-based approach for exact target localization in NLOS environments. Signal Process. 143, 328–335 (2018). https://doi.org/10.1016/j.sigpro.2017.09.019
12. Rousseeuw, P.J., Leroy, A.M.: Robust Regression and Outlier Detection. Wiley (1987)
13. Li, Z., et al.: Robust statistical methods for securing wireless localization in sensor networks. In: Proc. IEEE Int. Symp. Information Processing in Sensor Networks (IPSN), pp. 91–98. Los Angeles (2005)
14. Casas, R., et al.: Robust estimator for non-line-of-sight error mitigation in indoor localization. EURASIP J. Appl. Signal Process. 2006, 1–8 (2006). https://doi.org/10.1155/asp/2006/43429
15. Park, C.H., Chang, J.-H.: WLS Localization Using Skipped Filter, Hampel Filter, Bootstrapping and Gaussian Mixture EM in LOS/NLOS Conditions, pp. 35919–35928. IEEE Access (2019)
16. Park, C.H., Chang, J.-H.: Revisiting skipped filter and development of robust localization method based on variational Bayesian Gaussian mixture algorithm. IEEE Trans. Signal Process. 70, 5639–5651 (2022). https://doi.org/10.1109/tsp.2022.3224642
17. Chang, X.-W., Guo, Y.: 'Huber's *M*-estimation in relative GPS positioning: computational aspects. J. Geodesy 79(6-7), 351–362 (2005). https://doi.org/10.1007/s00190-005-0473-y
18. Hodges, J.L., Lehmann, E.L.: Estimates of location based on rank tests. Ann. Math. Stat. 34(2), 598–611 (1963). https://doi.org/10.1214/aoms/1177704172
19. Guvenc, I., et al.: NLOS identification and mitigation for UWB localization systems. In: Proc. IEEE Wireless Communications and Networking Conference, pp. 1571–1576. Kowloon, Mar. (2007)
20. Chan, Y.T., et al.: Time-of-arrival based localization under NLOS conditions. IEEE Trans. Veh. Technol. 55(1), 17–24 (2006). https://doi.org/10.1109/tvt.2005.861207
21. Park, C.H., Chang, J.-H.: Robust time-of-arrival source localization employing error covariance of sample mean and sample median in line-of-sight/non-line-of-sight mixture environments. EURASIP J. Appl. Signal Process., 1–11 (2016). Article ID 2016:89. https://doi.org/10.1186/s13634-016-0385-4
22. Gezici, S., Kobayashi, H., Poor, H.V.: Nonparametric nonline-of-sight identification. In: Proc. IEEE Vehicular Technology Conference, pp. 2544–2548. Mar., Orlando (2003)
23. Feng, Y., et al.: EM- and JMAP-ML based joint estimation algorithms for robust wireless geolocation in mixed LOS/NLOS environments. IEEE Trans. Signal Process. 62(1), 168–182 (2014). https://doi.org/10.1109/tsp.2013.2286779
24. Feng, Y., et al.: TOA-Based robust wireless geolocation and Cramér-Rao lower bound analysis in harsh LOS/NLOS environments. IEEE Trans. Signal Process. 61(9), 2243–2255 (2013). https://doi.org/10.1109/tsp.2013.2251341
25. Gustafsson, F., Gunnarsson, F.: Mobile positioning using wireless networks. IEEE Signal Process. Mag. 22(4), 41–53 (2005). https://doi.org/10.1109/msp.2005.1458284
26. Hammes, U., Wolsztynski, E., Zoubir, A.M.: Robust tracking and geolocation for wireless networks in NLOS environments. ' IEEE J. Sel. Top. Signal Process. 3(5), 889–901 (2009). https://doi.org/10.1109/jstsp.2009.2028383
27. Chen, B., et al.: Maximum correntropy Kalman filter. Automatica 76, 70–77 (2017). https://doi.org/10.1016/j.automatica.2016.10.004
28. Fakoorian, S., et al.: Maximum correntropy criterion Kalman filter with adaptive kernel size. In Proc. the IEEE National Aerospace and Electronics Conference (NAECON), pp. 581–584, (2019)
29. Liu, X., et al.: Maximum correntropy unscented Kalman filter for spacecraft relative state estimation. Sensors 16(9), 1–16 (2016). https://doi.org/10.3390/s16091530
30. Huang, Y., et al.: 'A Novel robust Student's t-based Kalman filter. IEEE Trans. Aero. Electron. Syst. 53(3), 1545–1554 (2017). https://doi.org/10.1109/taes.2017.2651684
31. Huang, Y., et al.: 'A novel robust Gaussian-Student's *t* mixture distribution based Kalman filter. IEEE Trans. Signal Process. 67(13), 3606–3620 (2019). https://doi.org/10.1109/tsp.2019.2916755
32. Huang, Y., et al.: A novel outlier-robust Kalman filtering framework based on statistical similarity measure. IEEE Trans. Automat. Control 66(6), 2677–2692 (2020). https://doi.org/10.1109/tac.2020.3011443
33. Ma, F., He, J., Zhang, X.: Robust Kalman filter algorithm based on generalized correntropy for ultra-wideband ranging in industrial environment. IEEE Access 7, 27490–27500 (2019). https://doi.org/10.1109/access.2019.2901940
34. Park, C.H., Chang, J.-H.: Robust localization based on non-parametric kernel technique. Electron. Lett. 58(22), 850–852 (2022). https://doi.org/10.1049/ell2.12625
35. An, X., et al.: Robust vehicle positioning based on multi-epoch and multi-antenna TOAs in harsh environments. IEEE Trans. Intell. Transport. Syst. 23(11), 21074–21089 (2022). https://doi.org/10.1109/tits.2022.3190023
36. Coluccia, A., Ricciato, F.: RSS-based localization via Bayesian ranging and iterative least squares positioning. IEEE Commun. Lett. 18(5), 873–876 (2014). https://doi.org/10.1109/lcomm.2014.040214.132781
37. Guo, X., Chu, L., Sun, X.: Accurate localization of multiple sources using semidefinite programming based on incomplete range matrix. IEEE Sensor. J. 16(13), 5319–5324 (2016). https://doi.org/10.1109/jsen.2016.2558184
38. Ho, K. C.: Bias reduction for an explicit solution of source localization using TDOA. IEEE Trans. Signal Process. 60(5), 2101–2114 (2012)
39. Jia, T., et al.: Target localization based on structured total least squares with hybrid TDOA-AOA measurements. Signal Process 143, 211–221 (2018)
40. Wang, G., Ho, K.C., Chen, X.: Bias reduced semidefinite relaxation method for 3-D rigid body localization using AOA. IEEE Trans. Signal Process 69, 3415–3430, (2021)
41. Jia, T., et al.: Mitigating sensor motion effect for AOA and AOA-TOA localizations in underwater environments. IEEE Trans. Wireless Commun 22(9), 6124–6139 (2023)
42. Kay, S.M.: Fundamentals of Statistical Signal Processing: Estimation Theory, vol. 1. Prentice Hall (1993)
43. Park, C.H., Chang, J.-H.: Robust localization method based on non-parametric probability density estimation. IEEE Access 11, 61468–61480 (2023). https://doi.org/10.1109/access.2023.3287140
44. Cappé, O., Moulines, E.: On-line expectation-maximization algorithm for latent data models. J. Roy. Stat. Soc. B 71(3), 593–613 (2009). https://doi.org/10.1111/j.1467-9868.2009.00698.x
45. Cappé, O.: Online EM algorithm for hidden Markov models. J. Comput. Graph Stat. 20(3), 728–749 (2011). https://doi.org/10.1198/jcgs.2011.09109
46. Mongillo, G., Deneve, S.: Online learning with hidden Markov models. Neural Comput. 20(7), 1706–1716 (2008). https://doi.org/10.1162/neco.2008.10-06-351
47. Cappé, O.: Online Expectation-Maximisation, pp. 1–53. Estimation and Applications', Mixtures (2011)
48. Surace, S.C., Pfister, J.: Online maximum-likelihood estimation of the parameters of partially observed diffusion processes. IEEE Trans. Automat. Control 64(7), 2814–2829 (2019). https://doi.org/10.1109/tac.2018.2880404
49. LeGland, F., Mevel, L.: Recursive estimation in hidden Markov models. In: Proc. 36th IEEE Conf. Decis. Control, pp. 3468–3473 (1997)
50. Sirignano, J., Spiliopoulos, K.: Stochastic gradient descent in continuous time. SIAM J. Financ. Math. 8(1), 933–961 (2017). https://doi.org/10.1137/17m1126825
51. Tadić, V.B.: Analyticity, convergence, and convergence rate of recursive maximum-likelihood estimation in hidden markov models. IEEE Trans. Inf. Theor. 56(12), 6406–6432 (2010). https://doi.org/10.1109/tit.2010.2081110

52. Bishop, C.M.: Pattern Recognition and Machine Learning. Springer (2006)
53. Xiong, W., et al.: TDOA-based localization with NLOS mitigation via robust model transformation and neurodynamic optimization. Signal Process., 178, pp, 1–10. (2021). https://doi.org/10.1016/j.sigpro.2020.107774
54. Radnosrati, K., Hendeby, G., Gustaffson, F.: Exploring positive noise in estimation theory. IEEE Trans. Signal Process. 68, 3590–3602 (2020). https://doi.org/10.1109/tsp.2020.2999204
55. O'Lone, C.E., Dhillon, H.S., Buehrer, R.M.: Characterizing the first arriving multipath component in 5G millimeter wave networks: TOA, AOA, and non-line-of-sight bias. IEEE Trans. Wireless Commun. 21(3), 1602–1620 (2022). https://doi.org/10.1109/twc.2021.3105641

How to cite this article: Park, C.-H., Chang, J.-H.: Robust localisation methods based on modified skipped filter weighted least squares algorithm. IET Radar Sonar Navig. 18(6), 825–837 (2024). https://doi.org/10.1049/rsn2.12526

APPENDIX

A | Derivation of Equations (40) and (41)

$\mathbf{F} = E\left[\left(\boldsymbol{\mu}_{b,1} - \mathbf{b}^o\right)\left(\boldsymbol{\mu}_{b,1} - \mathbf{b}^o\right)^T\right]$ from the definition of Equation (32). Then, $[\mathbf{F}]_{i,i} = E\left[\left(\mu_{b_i,1} - b_i^o\right)^2\right]$. That is, $[\mathbf{F}]_{i,i}$ denotes the MSE of $\mu_{b_i,1}$. The MSE is divided into the error variance and squared estimation bias. That is, $[\mathbf{F}]_{i,i} = \mathrm{Var}\left[\mu_{b_i,1}\right] + \left(E\left(\mu_{b_i,1}\right) - b_i^o\right)^2$. The $[\mathbf{F}^{\mathrm{CMS}}]_{i,i}$ is represented as the sum of error variance and squared estimation bias as follows:

$$\left[\mathbf{F}^{\mathrm{CMS}}\right]_{i,i} = \mathrm{Var}\left[\mu_{b_i,1}^{\mathrm{CMS}}\right] + \left(E\left(\mu_{b_i,1}^{\mathrm{CMS}}\right) - b_i^o\right)^2 \tag{A1}$$

First, $\mathrm{Var}\left[\mu_{b_i,1}^{\mathrm{CMS}}\right]$ is obtained as follows:

$$\mathrm{Var}\left[\mu_{b_i,1}^{\mathrm{CMS}}\right] = \mathrm{Var}\left[\frac{x_i^2 + y_i^2 - \left(\hat{r}_i^{\mathrm{MLE}}\right)^2}{2}\right] \tag{A2}$$

$$= \mathrm{Var}\left[\frac{x_i^2 + y_i^2 - d_i^2 - 2\left(\frac{d_i \sum_{j\in\mathrm{LOS}} n_{i,j}}{P_{\mathrm{LOS}}}\right) - \left(\frac{\sum_{j\in\mathrm{LOS}} n_{i,j}}{P_{\mathrm{LOS}}}\right)^2}{2}\right] \tag{A3}$$

$$= \mathrm{Var}\left[b_i^o - \frac{d_i \sum_{j\in\mathrm{LOS}} n_{i,j}}{P_{\mathrm{LOS}}} - \frac{\left(\sum_{j\in\mathrm{LOS}} n_{i,j}\right)^2}{2P_{\mathrm{LOS}}^2}\right] \tag{A4}$$

$$= \mathrm{Var}\left[\frac{d_i \sum_{j\in\mathrm{LOS}} n_{i,j}}{P_{\mathrm{LOS}}}\right] + \mathrm{Var}\left[\frac{\left(\sum_{j\in\mathrm{LOS}} n_{i,j}\right)^2}{2P_{\mathrm{LOS}}^2}\right] + \mathrm{Cov}\left(\frac{d_i \sum_{j\in\mathrm{LOS}} n_{i,j}}{P_{\mathrm{LOS}}}, \frac{\left(\sum_{j\in\mathrm{LOS}} n_{i,j}\right)^2}{2P_{\mathrm{LOS}}^2}\right) \tag{A5}$$

$$= \mathrm{Var}\left[\frac{d_i \sum_{j\in\mathrm{LOS}} n_{i,j}}{P_{\mathrm{LOS}}}\right] + \mathrm{Var}\left[\frac{\left(\sum_{j\in\mathrm{LOS}} n_{i,j}\right)^2}{2P_{\mathrm{LOS}}^2}\right] + \frac{d_i}{2P_{\mathrm{LOS}}^3} E\left[\left(\sum_{j\in\mathrm{LOS}} n_{i,j}\right)^3\right] \tag{A6}$$

$$= \frac{d_i^2 \sigma_1^2}{P_{\mathrm{LOS}}} + \frac{\sigma_1^4}{2P_{\mathrm{LOS}}^3} + \frac{d_i}{2P_{\mathrm{LOS}}^3}\left(\sum_{j\in\mathrm{LOS}} E\left[n_{i,j}^3\right] + 3\sum_{j\neq k} E\left[n_{i,j} n_{i,k}^2\right] + 6\sum_{j\neq k\neq l} E\left[n_{i,j} n_{i,k} n_{i,l}\right]\right) \tag{A7}$$

$$= \frac{d_i^2 \sigma_1^2}{P_{\mathrm{LOS}}} + \frac{\sigma_1^4}{2P_{\mathrm{LOS}}^3} + \frac{d_i}{2P_{\mathrm{LOS}}^3}\left(\sum_{j\in\mathrm{LOS}} E\left[n_{i,j}^3\right] + 3\sum_{j\neq k} E\left[n_{i,j}\right] E\left[n_{i,k}^2\right] + 6\sum_{j\neq k\neq l} E\left[n_{i,j}\right] E\left[n_{i,k}\right] E\left[n_{i,l}\right]\right) \tag{A8}$$

$$= \frac{d_i^2 \sigma_1^2}{P_{\mathrm{LOS}}} + \frac{\sigma_1^4}{2P_{\mathrm{LOS}}^3}. \tag{A9}$$

Next, the squared estimation bias of $\mu_{b_i,1}^{\mathrm{CMS}}$ is obtained as follows:

$$\left(E\left(\mu_{b_i,1}^{\mathrm{CMS}}\right) - b_i^o\right)^2$$

$$= \left(E\left[\frac{d_i\sum_{j=1}^{P_{\mathrm{LOS}}} n_{i,j}}{P_{\mathrm{LOS}}} + \frac{\left(\sum_{j=1}^{P_{\mathrm{LOS}}} n_{i,j}\right)^2}{2P_{\mathrm{LOS}}^2}\right]\right)^2 \tag{A10}$$

$$= \left(E\left[\frac{\left(\sum_{j=1}^{P_{\mathrm{LOS}}} n_{i,j}\right)^2}{2P_{\mathrm{LOS}}^2}\right]\right)^2 \tag{A11}$$

$$= \frac{\sigma_1^4}{4P_{\mathrm{LOS}}^2}. \tag{A12}$$

Finally, $[\mathbf{F}^{\mathrm{CMS}}]_{i,i}$ is obtained as the sum of error variance and squared estimation bias as follows:

$$\left[\mathbf{F}^{\mathrm{CMS}}\right]_{i,i} = \frac{d_i^2\sigma_1^2}{P_{\mathrm{LOS}}} + \frac{\sigma_1^4}{2P_{\mathrm{LOS}}^3} + \frac{\sigma_1^4}{4P_{\mathrm{LOS}}^2}. \tag{A13}$$

In the same manner, $[\mathbf{F}^{\mathrm{CS}}]_{i,i}$ can be calculated.

B | MSEs of d_i^{OMMS} and d_i^{OEMS} using the online methods and d_i^{GMMS} using the existing GMMS-WLS method

The error variance of the distance estimate of the OMMS-WLS method $\left(d_i^{\mathrm{OMMS}}\right)$ is asymptotically equivalent to the CRLB because the MLE is the asymptotically efficient (unbiased and attaining the CRLB) estimator [42]. Then, the MSE of d_i^{OMMS} can be represented as follows:

$$\mathrm{MSE}\left[d_i^{\mathrm{OMMS}}\right] \simeq -\frac{1}{\sum_{j=1}^{P} E\left[\frac{\partial^2 l_{i,j}}{\partial d_i^2}\right]} \tag{A14}$$

$$= \frac{1}{\sum_{j=1}^{P} \tau_{i,k'(j)}} \tag{A15}$$

$$= \frac{1}{\frac{P_{\mathrm{LOS}}}{\sigma_1^2} + \frac{P_{\mathrm{NLOS}}}{\sigma_2^2}} \tag{A16}$$

$$= \frac{\sigma_1^2}{P_{\mathrm{LOS}}} - \frac{\frac{P_{\mathrm{NLOS}}}{\sigma_2^2}}{\left(\frac{P_{\mathrm{LOS}}}{\sigma_1^2}\right)^2 + \frac{P_{\mathrm{NLOS}}}{\sigma_2^2}}. \tag{A17}$$

where $l_{i,j}$ in Equation (A14) denotes Equation (19).

Further, the error variance of the distance estimate of the OEMS-WLS method $\left(d_i^{\mathrm{OEMS}}\right)$ is represented from Equation (25) as follows:

$$\mathrm{Var}\left[d_i^{\mathrm{OEMS}}\right] = \mathrm{Var}\left[\frac{\sum_{j=1}^{P}\tau_{i,j}\left(r_{i,j} - b_{i,j}\right)}{\sum_{j=1}^{P}\tau_{i,j}}\right] \tag{A18}$$

$$= \frac{\sum_{j=1}^{P}\tau_{i,j}^2\tau_{i,j}^{-1}}{\left(\sum_{j=1}^{P}\tau_{i,j}\right)^2} \tag{A19}$$

$$= \frac{1}{\sum_{j=1}^{P}\tau_{i,j}}. \tag{A20}$$

The estimation bias of d_i^{OEMS} can be shown to be equal to zero with simple algebra. Therefore, the MSE of d_i^{OEMS} is represented as follows:

$$\mathrm{MSE}\left[d_i^{\mathrm{OEMS}}\right] = \frac{1}{\sum_{j=1}^{P}\tau_{i,j}} \tag{A21}$$

$$= \frac{1}{\frac{P_{\mathrm{LOS}}}{\sigma_1^2} + \frac{P_{\mathrm{NLOS}}}{\sigma_2^2}} \tag{A22}$$

$$= \frac{\sigma_1^2}{P_{\mathrm{LOS}}} - \frac{\frac{P_{\mathrm{NLOS}}}{\sigma_2^2}}{\left(\frac{P_{\mathrm{LOS}}}{\sigma_1^2}\right)^2 + \frac{P_{\mathrm{NLOS}}}{\sigma_2^2}}. \tag{A23}$$

Note that $\mathrm{MSE}\left[d_i^{\mathrm{OMMS}}\right]$ and $\mathrm{MSE}\left[d_i^{\mathrm{OEMS}}\right]$ are the same.

Meanwhile, the MSE of d_i^{GMMS} is obtained as follows:

$$\mathrm{MSE}\left[d_i^{\mathrm{GMMS}}\right] = \mathrm{Var}\left[\frac{\sum_{j=1}^{P}\gamma_{i,j}r_{i,j}}{\sum_{j=1}^{P}\gamma_{i,j}}\right] + \left(E\left[\frac{\sum_{j=1}^{P}\gamma_{i,j}r_{i,j}}{\sum_{j=1}^{P}\gamma_{i,j}}\right] - d_i\right)^2 \tag{A24}$$

where $\gamma_{i,j}$ denotes the posterior probability (responsibility) used in the existing GMM EM algorithm [52]. Then, the property that $\gamma_{i,j} \simeq 0$ when $r_{i,j}$ belongs to the outlier and $\gamma_{i,j} \simeq 1$ when $r_{i,j}$ belongs to the inlier is utilised. Subsequently, the $\mathrm{MSE}\left[d_i^{\mathrm{GMMS}}\right]$ is represented as follows:

$$\mathrm{MSE}\left[d_i^{\mathrm{GMMS}}\right] \simeq \frac{\sigma_1^2}{P_{\mathrm{LOS}}}. \tag{A25}$$

Therefore, the $\mathrm{MSE}\left[d_i^{\mathrm{OMMS}}\right]$ and $\mathrm{MSE}\left[d_i^{\mathrm{OEMS}}\right]$ are smaller than $\mathrm{MSE}\left[d_i^{\mathrm{GMMS}}\right]$.